



DESIGN AND PRODUCTION OF AUTOMATED CHARCOAL PRESSING IRON: LEVERAGING THERMOELECTRIC GENERATOR TECHNOLOGY FOR ENHANCED EFFICIENCY

Tommy, S. D^{*1}.,Aka, C. C². and Onah, T. O².

1 Transport and Auto Maintenance Department, Works and Engineering Services Division, AkanuIbiam Federal Polytechnic, Unwana, Ebonyi State.

2 Department of Mechanical and Production Engineering, Enugu State University of Science and Technology, Enugu State

Author for correspondence: Onah, T. O.; **Email:** okechukwu.onah@esut.edu.ng

Abstract: This work focuses on the design and development of an automated charcoal pressing Iron (ACPI). The concept leverages on thermoelectric generator (TEG) technology that harvests heat energy from charcoal combustion and uses the captured temperature differential between the burning charcoal in the combustion chamber (cc) of the pressing Iron and the external ambient environment to generate electricity which energizes a 5V DC mini blower fan that intermittently sends oxygen into the charcoal combustion chamber at the prompt of a heat sensor for maintenance and sustenance of the combustion process. The design which incorporates a thermostatic control system utilizes Three Dimensional Computer Aided Design (3D CAD) of Solidworks and Altium Designer software environments to facilitate ease of system components integration. Components production employs laminated object manufacturing (LOM) processes in the development of patterns for investment casting of the Soleplate embedded charcoal compartment unit, lid and handle base. Protective plating of key surfaces uses heat resistant ceramic composite for conductive heat loss reduction. The evaluated efficiency indicates that this designed ACPI is 68.3% more efficient than the traditional charcoal pressing Iron (TCPI). As a proposed household appliance in rural areas without electricity, this innovation offers a modern convenient alternative to the TCPI.

KEYWORD: Automated Charcoal Pressing Iron, Thermoelectric Generator, Low Watt Mini Fan, Thermostatic Control System, Enhanced Cloth Ironing Efficiency

1 Introduction

In many parts of the world, especially in rural areas and in regions where electricity is either unavailable or access to it is limited, traditional methods of ironing clothes using TCPI have persisted. The device are heated using burning wood charcoal thus providing a convenient and cost effective solution for achieving wrinkle free clothing. TCPI have a rich historical significance, dating back to the 19th century as they were widely used before the advent of electric irons, thus making the household appliance an ancestor to the modern Electric Pressing Iron (Mcgril, 2017).

The TCPI, commonly known as a “charcoal iron” or “box iron” is a traditional household

tool. Unlike modern electric irons that are powered by electricity, the TCPI is heated using burning charcoal placed inside it. Figure 1.0 shows a traditional charcoal pressing iron which is accessible in almost every market in developing countries. In the earliest days, people ironed their clothes using “sad iron” (SI) which was heavy bars with handles.



Fig. 1.1: Traditional Charcoal Pressing Iron

Today, there are several designs of charcoal iron in use especially in developing nations where there is either no electricity or the available source of electric power supply is either too expensive or unreliable. Inefficient heating and poor charcoal combustion management remain a serious challenge facing users of TCPI. However, in recent years, advancements in technology have led to the integration of renewable energy sources and smart systems into various household appliances aiming at enhancing efficiency and sustainability. Among these innovations, most steelworks industries now use TEGs to harvest electricity from waste heat (Kuroki *et al.*, 2014). Thus, the incorporation of TEGs into several appliances has gained significant attention due to their ability to convert heat energy into useful electricity (Zhang *et al.*, 2015).

Leveraging on the work of Rabiou *et al* (2020), the incorporation of a thermoelectric module to convert heat energy from charcoal iron into electrical power for energizing a mini fan for the maintenance of efficient combustion in an ACPI is a feasible enterprise. In this context, the application of TEGs in household appliances like this ACPI presents a unique opportunity to improve energy utilization and user experience (Fiksel, 2009). In the study of fan power effect on electrical output of a TEG used to enhance the combustion of wood charcoal in a combustion chamber of which the sidewalls were plated with thermoelectric modules while the cold side was a block filled with running water; Soumi *et al* (2023) observed that increase in fan power facilitated adequate combustion and increased the heat available to the cc, thus increasing the temperature difference of the TEG which resulted in an increase in the power output of

the device. More so, the integration of TEG module in a charcoal stove whose This work introduces the concurrent engineering design and development of an automated charcoal pressing iron embedded with a TEG, which harnesses self-heat, energy-converted electricity to power a mini blower fan intermittently, thereby maintaining combustion for continuous heating of the iron's soleplate to enhance clothes ironing efficiency.

Performance in electricity generation was simulated at different ambient temperatures revealed that TEG embedded in the self-powered naturally aspirated thermoelectric (TEC) charcoal stove generated electric voltage at ambient temperatures (Ajah, 2018). However, the work further revealed that the temperature of the heat sink (cold side of the TEG) imposes a great influence on the electric voltage that a TEG can produce, as the generated voltage decreases with the increase in ambient temperature.

1.2 The Design Concept

The conception, design and development of an ACPI system assembly as a household appliance for convenient clothes ironing efficiency in rural areas where there is no electricity is a new variant of the TCPI currently in use across regions with unreliable or complete lack of electric power supply. Its design, manufacturing and introduction into the market was executed using a comprehensive concurrent engineering approach to ensure a just in time delivery of the new variant of TCPI to target users. The approach involves integrating various phases of product development, such as initial concept, design and prototyping, manufacturing, facility set up, manufacturing operations, sales and delivery; to happen simultaneously rather than consecutively.

The ACPI was designed using basic principles of advanced metal casting manufacturing processes, TEG technology, heat transfer, thermostatic control operation and fan mechanics. This technology based product utilizes heat energy from the charcoal compartment to generate electricity using TEG. The electricity generated via temperature gradient is directed to energize a 5V DC blower fan affixed to the internal roof of the iron's lid. During operations, the fan intermittently blows air into the charcoal chamber to sustain combustion for continuation of heat generation and supply to the iron's soleplate which is used in furthering the clothes ironing process conveniently. This product offers efficient heat generation, controlled airflow and enhanced users experience during use.

1.3 Related Theories, Equations And Assumptions

The following related theories, equation and assumptions were reviewed.

1.3.1 Energy Efficiency Model

The second law of thermodynamics holds that efficiency of a Carnot Cycle can be calculated using Carnot efficiency formula:

$$\eta = 1 - \frac{T_c}{T_h} \quad (1.1)$$

where: η is the efficiency of the cycle;

T_c is the absolute temperature of the cold side ; and

T_h is the absolute temperature of the hot side temperature

1.3.2 Seebeck Effect

This is the electromotive force (emf) that is created across two points of materials that possess electrical conductivity when a temperature difference exists between them. The direct conversion of this temperature difference to electric voltage using a thermocouple is what is commonly referred to

as thermoelectric or Seebeck effect (Goupil *et al.*, 2016).

1.3.3 Seebeck Equation

The Seebeck equation describes the voltage generated due to the Seebeck effect. It connects by a linear relationship, the Voltage (V) and the temperature difference (ΔT) between the hot and cold sides of the TEG to the Seebeck coefficient (S) of the TEC material used in the design of the thermocouple system thus:

$$V = S \times \Delta T \quad (1.2)$$

A positive Seebeck coefficient (S), indicates that the voltage generation is in the same direction as the temperature gradient while a negative Seebeck coefficient shows that the voltage generation is in opposite direction of the temperature gradient (Siesta, 2005).

1.3.4 Seebeck Coefficient

Seebeck coefficient quantifies the ability of a material to generate a voltage difference when there is a temperature gradient across it (Wu *et al.*, 2017). It measures the ratio of the thermal e.m.f. produced as a result of the TEC effect to the corresponding, degree change in temperature across a junction of two metals that have distinct properties. The Seebeck coefficient measures the magnitude of the induced TEC voltage which results from the temperature difference between two junctions.

1.3.5 Dimensionless Figure of Merit

The dimensionless figure of merit (ZT) of a TEC material is defined as the ratio of the desired energy gained to the energy input (Sestak, 2005). Bismuth telluride (Bi_2Te_3) and its derivatives (Bi-Te) among other TEC materials exhibit very high ZT values at near room temperature. They manifest great potential when evaluated side by side with other TEC materials (Cao *et al.*, 2023). The determination of the performance of TEGs and TECs is anchored on the ZT which Beretta *et al.* (2019) defined as:

$$ZT = \frac{S^2 \sigma}{K} T = \frac{S^2}{K_e + K_l} T \quad (1.3)$$

Where: S is the Seebeck coefficient, σ is the electrical conductivity, $S^2 \sigma$ is the power factor, K_e is the electrical thermal conductivity, K_l is the lattice thermal conductivity; and T is the absolute temperature.

In practical application such as this work, Cao *et al* (2023) noted that average dimensionless figure of merit (ZT_{ave}) is precisely an efficient way of evaluating the performance of a Bi_2Te_3 TEG system and gives an expression for the average ZT as:

$$ZT_{ave} = \frac{\int_{T_c}^{T_h} ZT dT}{T_h + T_c} \quad (1.4)$$

According to Synder *et al* (2017), it is precisely a huge challenge to vividly describe the energy conversion efficiency (η_{ec}) and the coefficient of performance (COP) of any TEG device. However, Cao *et al* (2023) defines η_{ec} and COP thus:

$$\eta_{ec} = \frac{T_h - T_c}{T_h} \times \frac{\sqrt{1 + ZT_{dev}} - 1}{\sqrt{1 + ZT_{dev}} + \frac{T_c}{T_h}} \quad (1.5)$$

$$COP = \frac{T_c}{T_h - T_c} \times \frac{\sqrt{1 + ZT_{dev}} - \frac{T_h}{T_c}}{\sqrt{1 + ZT_{dev}} + 1} \quad (1.6)$$

Where: ZT_{dev} is the dimensionless figure of merit of the device.

In Synder *et al* (2017), the dimensionless figure of merit, ZT is defined for a TEG using the maximum efficiency of the TEC device calculated from exact equation (1.5), thus:

$$ZT = \left(\frac{T_h - T_c(1 - \eta_{ec})}{T_h(1 - \eta_{ec}) - T_c} \right)^2 \quad (1.7)$$

A higher ZT indicates better performance and ZT increases from 0.8 to 1.18 as temperature increases from 24.85°C to 176°C (Goldsmid, 2014). In order for the performance of Bi-Te TEC device to be accurately evaluated, certain parameters including open circuit voltage

(V_{oc}), output power (P) and power density (ω) ought to be known. As defined by Zhang *et al* (2015) and Hou *et al* (2018), the parameters are mathematically expressed thus:

$$V_{oc} = n(S_p - S_n) \times (T_h - T_c) \quad (1.8)$$

$$P = \frac{V_{oc}^2}{R_{in} + R_{load}} \times R_{load} \quad (1.9)$$

$$\omega = \frac{P}{A_c} = \frac{(T_h - T_c)^2}{4L} \times S^2 f \sigma \quad (1.10)$$

Where: n is the number of TEC materials;

S_p and S_n are seebeck effect (S) of the P- and N- type materials; R_{in} and R_{load} are the internal resistance and load resistance of the TEC devices respectively; A_c is the cross section within the Bi-Te based Thermoelectric Device (TED) and f is the fill factor within these TEDs. Thus, V_{oc} , P and ω are material's properties which have inherent relationships.

1.3.6 Thermal Energy Equation

Thermal energy equation is given by:

$$Q = MC_p \Delta T \quad (1.11)$$

Where: Q is the heat transfer

M is mass of the substance

ΔT is the temperature change or gradient,

C_p is the specific heat capacity.

1.3.7 Heat Transfer Analysis

Conductive heat transfer analysis to determine the heat flow from the charcoal to the TEG and the iron's soleplate can be done using Fourier's law of heat conduction below:

$$Q = -k \times A_c \times \frac{dT}{dx} \quad (1.12)$$

where: Q is the heat transfer rate,

k is the thermal conductivity of the material,

A_c is the cross sectional area of the heat transfer, and $\frac{dT}{dx}$ is the temperature gradient.

Thermal conductivity measures how well a material conducts heat. In order to reduce the loss of heat and improve the heat-to-electricity

conversion efficiency in thermoelectric applications, a low thermal conductivity is required. Bi-Te materials possess a low thermal conductivity in the range of 1 to 2W/(m.K) (Kim *et al.*, 2010). The work of Kim *et al* (2010) and Goldsmid (2014) give electrical resistivity, Seebeck effect and thermal conductivity of Bi₂Te₃ as $0.6 \times 10^{-5} \Omega m$, $160 \mu V/K$ for P-type, $-170 \mu V/K$ for n-type materials and $1.3 W m^{-1} K$ respectively; The electrical conductivity of $1.1 \times 10^5 S.m/m^2$ and low lattice thermal conductivity of 1.20W/9m.k) are also inherent properties of Bi₂Te₃ (Cao *et al.*, 2023).

1.3.8 Heat Sink

The volumetric thermal resistance of the heat sink guarantees dissipation of heat from the Peltier element to the ambient air with the help of natural convection and aspiration. In practice, heat dissipation via convection is calculated thus:

$$Q = a_c \times A_s \times \Delta T \quad (1.13)$$

Where: a_c is the convective heat transfer coefficient; and A_s is the surface area of the heat sink.

1.3.9 Thermostatic Control Model

The design of a control system that uses a thermostat to maintain a desired temperature on the iron's combustion chamber and the soleplate involves feedback control theory and concepts like Proportional – Integral – Derivative (PID) control. The PID equation is:

$$u(t) = k_p \times e(t) + K_i \times \int_0^t e(\tau) d\tau + K_d \times \frac{de(t)}{dt} \quad (1.14)$$

where: $u(t)$ is the control input (fan speed in this case), $e(t)$ is the error (difference between desired and actual temperature),

k_p , K_i and K_d are the PID gains and t is the time.

1.3.10 Charcoal and Textile/Fabric Properties

The burn rate of naturally aspirated wood charcoal ranges from 0.002766g/min to 11.5g/min depending on the wood quality, type and moisture content and has energy content of 29000J/g (Ajah, 2018; Hassan *et al.*, 2017; Lubwama *et al.*, 2021; Nurba *et al.*, 2019 and Olusegun *et al.*, 2014). Most cloths being used by humans are made of textile materials and the heat capacity of textile ranges from 0 to 3kJ/kg/K (Sharper *et al.*, 2017 and Spencer-Smith, 2008). The thermal conductivity of textiles (linen) is given as 0.188W/mK (Bethan, 2022). During normal clothes ironing operations, the soleplate temperature of pressing irons goes through three levels of temperatures; namely: low temperature, medium and high temperatures of 90°C - 120°C, 120°C - 160°C and above 160°C respectively (Shuawei.com). Similarly, wood charcoal burns at low temperature, carbonization temperature and high temperature of 300°C, 600°C and above 1020°C respectively (Lubwama *et al.*, 2021 and Opensaw, 2009). In his work, Mage (2006) determined the density of charcoal to be at the range of 180 to 220kg/m³.

2 Materials and Method

2.1 Initial Concept and Market Survey

A thorough market survey was conducted in the rural areas of Ebonyi, Enugu, Abia, Imo and Anambra States of Southeast Nigeria where there is epileptic electric power supply from the national grid. The rural dwellers use electricity they generate from gasoline Generators to meet their electric power needs. Consequent upon the removal of petrol subsidy and the high cost of premium motor spirit (PMS), generation of electricity via gasoline Generators to meet the huge power demand for undertaking domestic chores like ironing of clothes has becomes a major

challenge. The market survey revealed the willingness of proposed users to pay for an automated system that utilizes locally sourced fuel input for ironing of clothes other than the conventional electric iron and the traditional CPI.

2.2 Definition of Product Specifications

The features of the ACPI are embedded TEC, low watt fan, thermostatic and intermittent blowing mechanism, durability, ease of use and safety.

(a) Fan Control Strategy:

A control strategy for the mini fan was based on the thermostat's output which involved using on-off control based on a hysteresis band around the set temperature. The blowing mechanism is based on simple mechanical linkage and gears.

(b) Charcoal Combustion Model:

A simplified model that predicts the rate of charcoal combustion based on airflow, temperature, and chemical properties of charcoal was incorporated which involves empirical equations derived from the experimentation.

(c) Overall System Energy Balance:

An energy balance equation for the entire system was developed taking into consideration the heat transfer, electricity generation and consumption by the mini fan; and losses. This equation will help to ensure that the system operates efficiently and predict the overall performance.

(d) Simulation and Iterative Design:

Numerical simulations were utilized to model the behavior of the entire system under various conditions which aided in optimizing the design parameters, such as TEG size, fan characteristics, and thermostatic settings.

2.3 Design Concept and Prototyping:

(a) Component Selection:

- High quality cast iron was selected for the pressing iron's Soleplate embedded

charcoal compartment unit, lid and handle base for durability.

- A Bi-Te based module designed for power generation from high temperature heat source which operates continuously at 330°C and intermittently up to 400°C was chosen for the TEG system of the Iron and was procured online from TEGMART.com at the cost of 5,739.46NGN. The TGPR-22W-7V-56S TEG Module has high conductive graphite sheets on both sides of the ceramic plates to provide the required low thermal resistance such that no additional thermal grease was required during installation (Tecpro, na).
- The TEGMART TE-HS Aluminum Heat Sink block on fig. 2.4 was also procured online from TEG.
- A 5V DC fan optimized for intermittent operation with easy thermal heat dissipation and low noise features available online (konga.com) at the cost of 1,750NGN was selected for charcoal combustion compartment blow function application.

(b) Prototype Development:

- A 3D CAD model of the concept was created as in fig.2.5 and the product behavior simulated in a CAE software environment.
- Design of electrical components and circuit diagram were done using Altium designer with electronic components library add-in.

(c) Testing and Iteration:

- Performance tests were conducted to ensure efficiency of the thermoelectric generator (TEG). Prior to assembly, the TEG, fan, and iron's soleplate were tested and the system fine-tuned for efficiency and safety.

- Design Revision Iteration Scheme was carried out thus: Conceptual Design → Materials Selection → Prototype Construction → Field Testing → Data Analysis → Challenges Identification → Iterative Improvement → Prototype Iteration → Repeat Testing → Refinement Continuation → User Feedback → Scalability and Sustainability → Education and Training → Documentation.
- Design was optimized based on the results of the tests for improved performance and usability.

(d) Component Parts And Functions

The parts and functions are as follows:

- Thermoelectric Generator (TEG) in fig. 2.1 converts the thermal heat generated by burning charcoal into electrical energy using See-beck effect and table 2.1 shows the module's data sheet.



Fig. 2.1: TEGPR-22W-7V- 56 TEG Module

Table 2.1: Thermoelectric Generator Module Data

Sheet.Source:<https://www.tegmart.com/index.php?>

Parameters	Ratings
Hot Side Temperature (°C)	300
Cold Side Temperature (°C)	30
Open Circuit Voltage (V)	14.4
Matched Load Resistance (ohms)	2.4
Matched Load Output Voltage(V)	7.2
Matched Load Output Current (A)	3.0
Matched Load Output Power (W)	21.6
Heat Flow across the Module (w)	≈ 415
Heat Flow Density (w/cm ²)	≈ 13.2

- Blower Fan on fig. 2.2 provides controlled airflow to enhance charcoal combustion by increasing oxygen supply to the cc and regulating the temperature of

the burning charcoal which helps maintain consistent and optimal heat levels for ironing. The fan is embedded with a control mechanism which links to the temperature sensor for automatic adjustment and intermittent operation of the Blower Fan to ensure controlled airflow for efficient combustion.

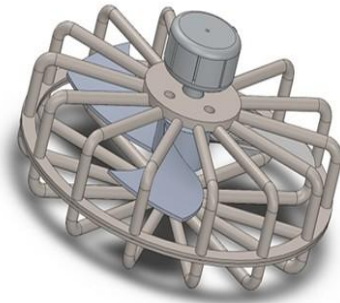


Fig. 2.2: Solidworks Drawing of 5V DC Brushless Cooling Fan Assembly

Table 2.2: Data Sheet of 5v Dc BlowerFan

Parameters	Ratings
Voltage (V)	5V
Current (I)	0.126A
Power (P)	14.4
CMF	3.6
RPM	9000
Noise	25DBA

- Charcoal Compartment – Soleplate Unit in fig. 2.3 is a multi-function unit which holds the charcoal securely and ensures controlled airflow to the charcoal through the base vent fixtures. The orange color arrow points to the combustion chamber and the blue arrow points to the Soleplate's flat area which receives heat used for ironing cloths by direct contact movement with the fabric.

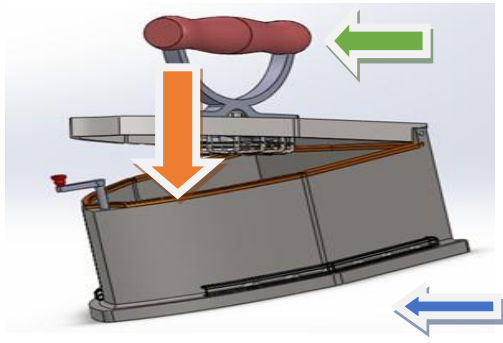


Fig. 2.3: Axonometric view of the CAD Model showing Charcoal Compartment

- iv. **Handle:**The green arrow on fig. 2.3 points to the device's handle which provides a grip for the user to hold and maneuver the ironing processes. It is made of heat-resistant wood for safe handling.
- v. **Temperature Sensor:**This unit is incorporated into the fan's Printed Circuit Board (PCB) on fig. 2.10 and monitors the temperature of the device's combustion chamber by adjusting the airflow for charcoal combustion maintenance and safe ironing temperature.
- vi. **Air Vent Fixture:**This fixture on the base of the Soleplate-charcoal compartment unit as shown by the yellow arrow on fig. 2.5 allows air to circulate within the charcoal compartment of the Iron to provide adequate oxygen required for combustion as well as serving as an exit channel for expulsion of burnt gases.
- vii. **Heat Sink** displayed on fig. 2.4 ensures heat dissipation from the TEG module thus maintaining a safe operation within temperature limits.

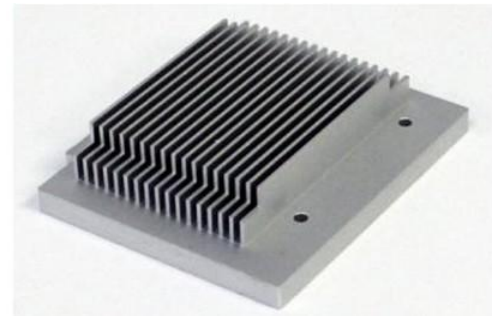


Fig. 2.4: TEGMART TE-HS Aluminum Heat Sink block procured online from Tegmart.com

- viii. **Hinges or Pivot:**Allows the user to press down the soleplate onto the fabric while ironing. It also enables user to open the Iron's lid to add charcoal and ignite the initial flame required.

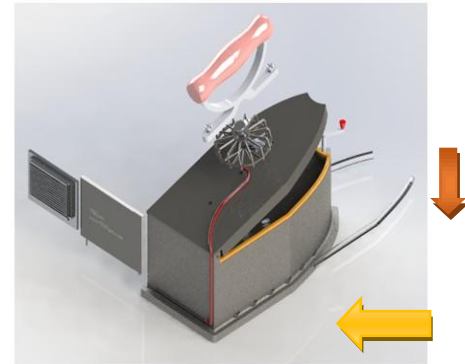


Fig. 2.5: Exploded view of the CAD model

- ix. **Ash Tray:**As the charcoal burns, it produces ash. This compartment indicated by the brown arrow on fig. 2.5 collects the ashes, keeping it separate from the clothing.
- x. **Lock Mechanism:**This important part indicated by the black and white arrow on fig. 2.6 is the mechanism that secures the Lid and keeps the assembly in a closed position.

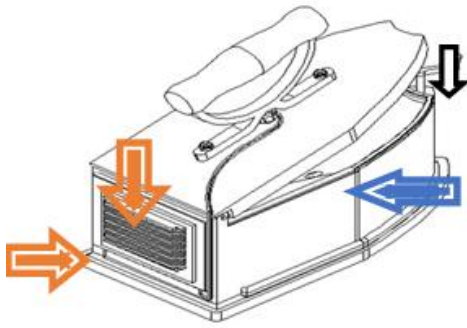


Fig. 2.6: Isometric view of the assembly

- xi. **Square Ceramic Fibre Insulator:** Serves as an insulator between the lid and the charcoal chamber of the iron. It seals the lid door to facilitate heat retention within the charcoal combustion chamber during ironing application. The location of this thermal heat-resistive insulator is as pointed by the blue arrow on fig.2.6.

Lid Top and Iron Rear Insulators: This is a ceramic fibre board with low heat conductivity at high temperature (1260°C) and has resistance to high gas velocity. Its function is to prevent radiation heat conduction and maintain temperature differential between the heat sink and the hot side of the TEG (located as pointed by the orange arrows on fig. 2.6).

Other pictorial views of the design concept are as displayed on fig. 2.7 and fig.2.9. Table 2.1 shows the labeling of the device's parts location as on the balloon drawing of fig. 2.9 while fig.2.10 shows the configuration of the electrical system.

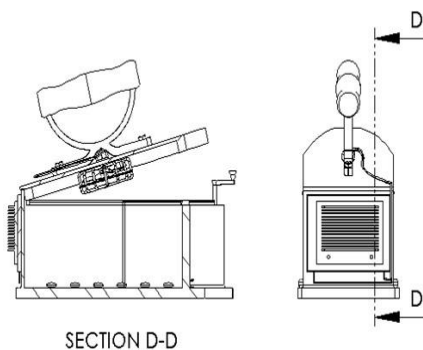


Fig. 2.7: Sectioned view (revealing location of the blower)

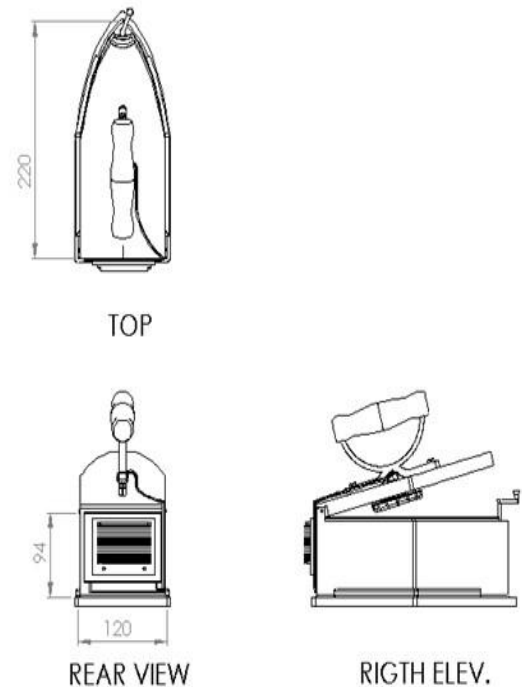


Fig. 2.8: Standard 3 Orthogonal Views

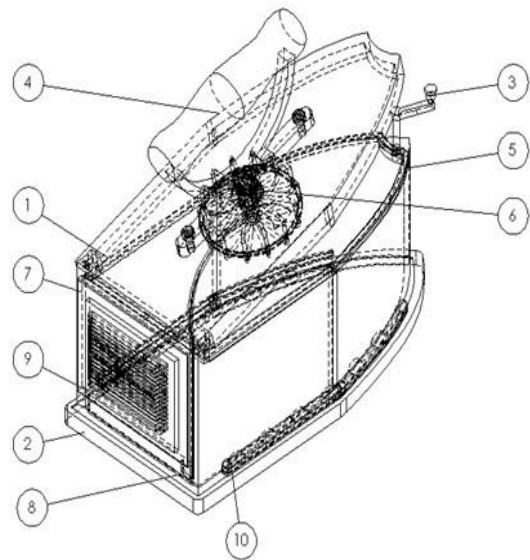


Fig. 2.9: Ballooned drawing (hidden details visible)

Table 2.3: Part List

ITEM NO.	PART NUMBER	DESCRIPTION	QTY
1	001	Lid	1
2	002	Soleplate Charcoal Chamber Unit	1
3	003	Lock	1
4	004	Handle	1
5	005	Rim Insulator	1
6	006	Fan Assembly	1
7	007	TEG	1
8	008	Wire	1
9	009	Heat Sink	1
10	005	Ash Tray	1
11	003	Fastener - Screw	2

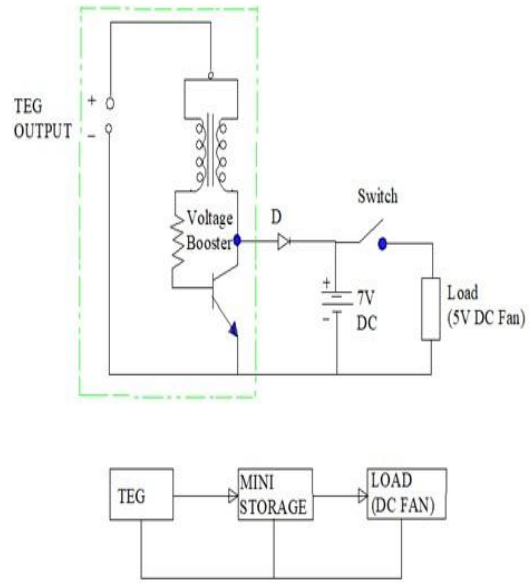


Fig. 2.10: Electrical Configuration of the Pressing Iron

Manufacturing Facility Setup

Facility Design and Setup:

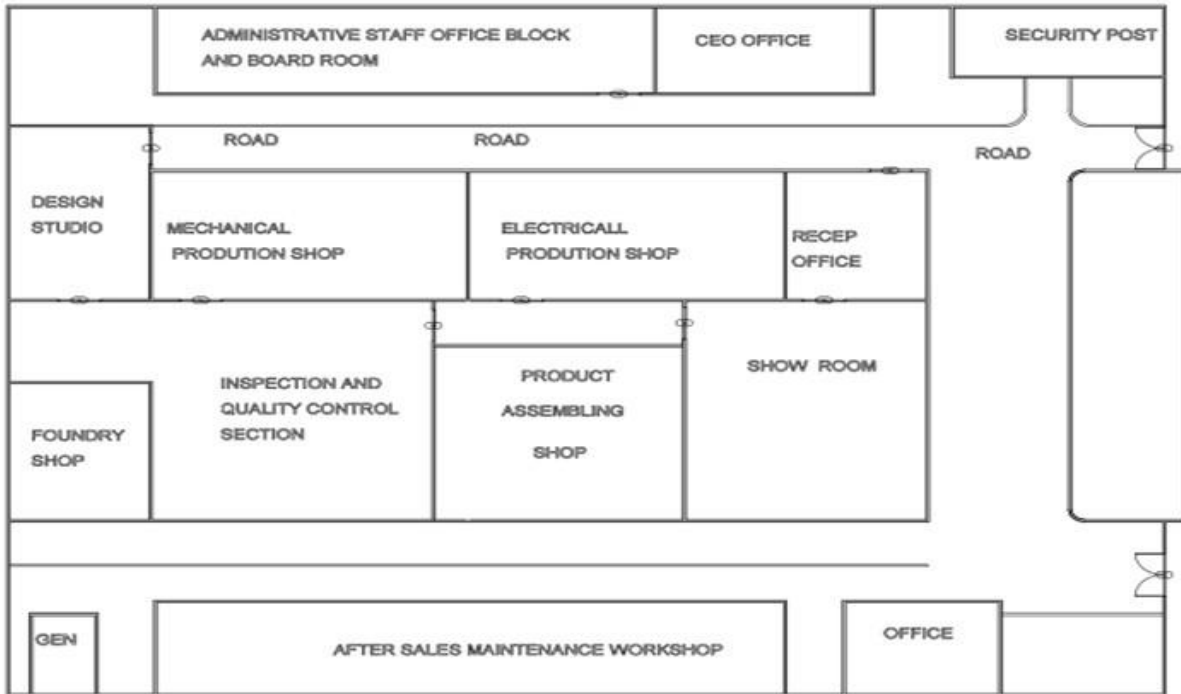


Fig. 2.11: Design layout of manufacturing facility

i. A manufacturing facility in a low cost-effective location of Agbani in Enugu State was established. The necessary machinery and equipment were acquired, installed and

skilled manpower for functional operations was engaged. The design layout of manufacturing facility is as on fig. 2.11.

ii. Quality Control and Process Validation: Strict quality control procedures were implemented and production processes were validated by regulatory agencies including SON and COREN.

(e) Manufacturing Operations:

i. Materials Procurement:

Materials were sourced and procured in bulk to reduce costs.

ii. Production and Assembly:

The produced automated CPI's components were assembled efficiently as follows:

❖ The TEG was securely attached to the rear of the charcoal iron as on the design prototype and the cold side fitted with the heat sink thus ensuring a good thermal conductivity for efficient heat transfer.

❖ The wire of the TEG's electrical output was connected to the Voltage Booster which is to boost the voltage generated by the TEG to become useable by the fan. The voltage booster has a capacitor bank to store electrical energy and to a diode to prevent reverse current flow.

❖ The output of the voltage booster was connected to the 5V DC blower fan.

❖ All the connections were secured and insulated properly to prevent heat-related damage.

❖ The TEG, fan, wiring, and electrical components were packed in an enclosure of heat-resistant housing to protect them from dust and moisture.

iii. Quality Control and Assurance:

Quality control checks were performed at various stages of the production and the reliability of the product was assured.

(f) Proposed Sales and Delivery

(g) Marketing and Distribution:

Marketing strategies were developed for rural areas and distribution channels were established to ensure just in time delivery of the product to target users.

i. Costing:

The costs of materials, labor, overhead and transportation including marketing and distribution expenses were calculated.

ii. Pricing:

A competitive yet profitable price based on cost and market analysis was set for the product.

iii. Volume Estimation:

Annual sales volume was estimated based on market research.

(h) Projected Costs Analysis, Determination of Unit Cost and Anticipated Sales:

i. Anticipated Volume of Annual Sales: 30,000 units in the first year and gradually increasing to about 50,000 per year over five (5) years as awareness and demand grows. Two (2) years tax and rates holidays/relief considered for this proposal

ii. Manufacturing Cost per unit: ₦ 15,513.33

iii. Marketing Margin per unit: ₦ 1000.00

iv. Distribution Margin per unit: ₦ 1,000 .00

Table 2.4: Details of Costs of Design and Development

Expenditures	Cost (₦ : K)	Total (₦:K)
✓ Initial Development Costs		
Market Survey and Research	200,000.00	
Design and Prototyping	100,000.00	
Intellectual Property Protection and Patent	100,000.00	
Regulatory Approvals (CAC, COREN,SON)		
Sub Total		550,000 .00
✓ Manufacturing and Operations Costs		
Manufacturing Facility Setup	20,000,000.00	
Raw Materials @ ₦12,000.00 per unit	390,000,000.00	
Labour and Overhead @ ₦1,500.00 per unit	45,000,000.00	
Quality Control and Testing @ ₦ 100.00 per unit	3,000,000.00	
Packaging @ ₦ 200.00 per unit	6,000,000.00	
Sub Total		434,000,000 .00
✓ Marketing, Sales, and Delivery Costs		
Marketing and Promotion	300,000 .00	
Distribution Network Setup	300,000 .00	
Sales Team and Training	250,000 .00	
Sub Total		850,000 .00
Total Design and Production Costs		465,400,000 .00

(i) **Business Cashflow**

The details of the process business cash flow are as on the Spreadsheet of Appendix “A”.

2.4 Business Management Tools

The concurrent engineering design, production and sales of the ACPI were aided by the use of specific business management tools. Recruitments of staff, services records, attendance and payroll was made easy via the use of BambooHR human resource software application while Oracle Enterprise Resource Planning (Oracle ERP) application which integrates and streamlines production planning, inventory management, procurement and accounting were utilized to plan production schedules, resources optimization and production workflows management was also utilized during the ACPI manufacturing stages. The MasterControl quality control and assurance tool designed to suit the peculiar need of the company was employed to ensure product

quality with respect to set standards. To achieve a just in time delivery of the ACPI to the target users, an E-commerce and sales platform was managed online using Spotify software which made the online store and sales of the product efficient. For customer services, HotSpot customer relationship software application was integrated into the customer relationship and after sales support services for effective representation of the company before customers as well as solve the eminent needs of customers. DocuWare data protection software was specially designed with customization and incorporated into the database of the company to secure online operations and manage technical information with reliable backup storage systems.

2.5 Environmental Protection Strategies

The preliminary impact assessment conducted provided a reliable guide for the

execution of the manufacturing processes in line with global best practices. Some of the strategies implemented were the optimization of resources to reduce waste, the adoption of a renewable energy plan to minimize the emission of greenhouse gases and the incorporation of a waste recycling plant along production line to limit waste generation. More so, emission control systems were installed to capture and treat pollutants that emanate from the production processes in consonance with environmental safety regulations. The host community was engaged with the firm's management to foster a peaceful culture of mutual coexistence throughout the manufacturing and supply chain activities. These measures were interwoven and synergized to enhance the promotion of a safe environment and reduction of negative impacts for the realization of the organizational goals of sustainable and long term manufacturing and distribution of the ACPI.

3 Results and Discussions

This work considered heat conduction in the charcoal compartment of the pressing iron's thickness as lossless, and evaluated the efficiency and coefficient of performance of the system based on data obtained from the testing of the product.

The automated charcoal pressing Iron was allowed to run optimally at an average hot side and cold side temperatures of 300°C and 30°C respectively for 30 minutes. Combustion in the charcoal compartment was in addition to the naturally aspirated air assisted with a plastic hand fan until the incorporated TEG generated sufficient voltage that energized the mini blowing fan to efficiently maintain a consistent

combustion process inside the charcoal compartment.

As designed, the charcoal pressing Iron has a combustion compartment volume of $2.85 \times 10^{-3} m^3$. The charcoal specimen used for the simulation of this work has a specific capacity of 1kJ/kg/K (The Engineering Toolbox, 2003) and a measured density of $208 kg/m^3$.

The initial mass of the charcoal loaded in the charcoal compartment of the Automated Charcoal Pressing Iron = 0.58kg

3.1 Thermal Energy of Charcoal

From equation (1.11) in the literature, thermal energy (Q_c) is given as:

$$Q_c = MC_p \Delta T$$

$$= 0.58kg \times 573.15 \times 1kJ/kgK$$

$$= 332.43 KJ$$

3.2 Thermal Power(P_{ci}) of Charcoal for 30 Minutes of Combustion Time

$$P_{ci} = \frac{Q_c}{t}$$

Where: t is the time of operation.

$$P_{ci} = \frac{332.43KJ}{1800 s} = \frac{(332.43 \times 1000)J}{1800 s} = 184.68W$$

3.3 Determination of Burn Rate of Charcoal in Traditional Charcoal Pressing Iron

Initial Mass of Charcoal (M_{ci}) = 0.58kg

Final Mass of Charcoal (M_{cf}) after 1800 seconds of combustion = 0.499kg

Burn Mass of Charcoal = Initial Mass – Final Mass

$$= 0.58kg - 0.499kg$$

$$= 0.081kg$$

$$\text{Burn Rate} = \frac{\text{Burn Mass}}{\text{Time}} = \frac{0.081kg}{1800 s} = 0.000045kg/s.$$

3.4 Calculation of Fire Power (W) of Traditional Charcoal Pressing Iron

$$\text{Thermal Fire Power (W)} = \frac{(M_{ci} - (M_{cf}) \times H_c}{\text{Ironing Time}}$$

where H_c is the energy content of charcoal (29000J).

$$W = \frac{(0.58\text{kg} - 0.499\text{kg}) \times 29000}{1800 \text{ s}} = \frac{(0.081 \times 1000)\text{J} \times 29000\text{J}}{1800 \text{ s}} = 1305\text{W}$$

3.5 Determination of Burn Rate of Charcoal in Automated Charcoal Pressing Iron

Initial Mass of Charcoal (M_{ci}) = 0.58kg

Final Mass of Charcoal (M_{cf}) after 1800 seconds of combustion = 0.13kg

Burn Mass of Charcoal = Initial Mass – Final Mass

$$= 0.58\text{kg} - 0.13\text{kg} \\ = 0.45\text{kg}$$

$$\text{Burn Rate} = \frac{\text{Burn Mass}}{\text{Time}} = \frac{0.45\text{kg}}{1800 \text{ s}} =$$

0.00025kg/s

3.6 Calculation of Fire Power (W) of the Automated Charcoal Pressing Iron

Fire Power (W) = $\frac{(M_{ci} - (M_{cf}) \times H_c}{\text{Ironing Time}}$; where H_c is the energy content of charcoal (29000J).

$$W = \frac{(0.58\text{kg} - 0.13\text{kg}) \times 29000}{1800 \text{ s}} = \frac{(0.45 \times 1000)\text{J} \times 29000\text{J}}{1800 \text{ s}} = 7250\text{W}$$

3.7 Thermal Efficiency of Charcoal Combustion

Applying Carnot efficiency formula in equation (1) of literature,

$$\text{Thermal Efficiency } (\eta_{\text{thermal}}) = 1 - \frac{303.15\text{K}}{573.15\text{K}} \\ = 1 - 53 = 0.47$$

$$\eta_{\text{thermal}} = 47\%$$

3.8 Seebeck Coefficient of TEG

From data Sheet of table 2.1

The voltage and Seebeck coefficient of TEG is related in conformity with equation (1.2).

Thus, Seebeck coefficient (S) of the TEG gives:

$$S = \frac{V}{\Delta T} = \frac{(V_{oc} - V_{load})}{\Delta T} = \frac{14.4\text{V} - 7.2\text{V}}{543.15\text{K}} = 0.013256\text{V/K}.$$

3.9 Dimensionless Figure of Merit of TEG

Based on information of Tecpro (na); Goupil *et al* (2016) and Goldsmid (2014), applying equation (1.3) yields:

$$ZT = \frac{(0.013256 \text{ v/k})^2 \times (1.1 \times 10^5 \text{ s/m}) \times 573.15\text{k}}{1.20\text{w/(m.k)}} = 1.3036$$

3.10 Energy Conversion Efficiency of TEG

From equation (1.5), the energy conversion efficiency (η_{ec}) of the TEG yields:

$$\eta_{ec} = \frac{573.15\text{K} - 303.15\text{K}}{573.15\text{K}} \times \frac{\sqrt{(1 + 1.3036) - 1}}{\sqrt{(1 + 1.3036 + \frac{303.15\text{K}}{573.15\text{K}})}} \\ = 0.4710808689 \times 0.6783998606 \\ = 0.3195811958 \\ = 31.958\%$$

Energy conversion efficiency of TEG (η_{ec}) = **32%**

3.11 Coefficient of Performance of TEG

Applying equation (6), the coefficient of performance of the TEG (COP_{TEG}) gives:

$$\text{COP}_{\text{TEG}} = \frac{303.15\text{K}}{573.15\text{K} - 303.15\text{K}} \times \frac{\sqrt{(1 + 1.3036 - \frac{573.15\text{K}}{303.15\text{K}})}}{1 + 1.3036 + 1} \\ = 1.122777778 \times 1.148193723 \\ = 1.289166397$$

$$\text{COP}_{\text{TEG}} = 1.3$$

3.12 Highlight of Energy Analysis of Automated Charcoal Pressing Iron

The energy input, losses and energy out of the system and processes are highlighted as follows:

- Power generated by the thermal combustion process = 7250W
- Power available due to thermal efficiency of the system (47%) = 3407.5W

- Power loss due to thermal efficiency of the system (53%) = 3842.5W
- Power used by Soleplate of Charcoal Pressing Iron = 1500W
- Power loss during TEG energy conversion {68% of (3407.5-1500)} = 1297.1W
- Energy available for conversion to electricity {32% of (3407.5-1500)} = 610.4W
- Energy loss due to Heatsink volumetric heat dissipation via convection = 588.17W
- Power used by TEG = 21.6W
- Power used by blower Fan = 0.63W

3.13 Energy Balance of Automated Charcoal Pressing Iron

- The energy balance (Q_{balance}) of a system is given by the expression:
- $Q_{\text{balance}} = Q_{\text{in}} - Q_{\text{out}} = 0$
- where: Q_{in} and Q_{out} are energy input and output respectively. From the energy analysis of the system;
- $Q_{\text{in}} = P_{\text{thermal}} = 7250\text{W}$
- $Q_{\text{out}} = P_{\text{Iron}} + P_{\text{teg}} + P_{\text{fan}} + P_{\Sigma\text{losses}}$
- $= 1500\text{W} + 21.6\text{W} + 0.63\text{W} + 3842.5\text{W} + 1297.1\text{W} + 588.17\text{W} = 7250\text{W}$
- $Q_{\text{balance}} = 7250\text{W} - \{1500\text{W} + 21.6\text{W} + 0.63\text{W} + 3842.5\text{W} + 1297.1\text{W} + 588.17\text{W}\} = 0$
- From the foregoing computation, it could be inferred that energy losses into the atmosphere via exhaust (vents), radiation through the Iron sidewalls, intentional dissipation through the incorporated Heatsink; and conductive heat losses through electrical resistance of wires and fan coils account for the

losses of the generated energy, Q_{in} . This is consistent with the ideal Carnot cycle heat losses and therefore indicates that the performance of the Automated Charcoal Pressing Iron operates in conformity with performance of a typical Carnot cycle engine operating between 15°C and 800°C temperature reservoirs.

3.14 Efficiency of Traditional Charcoal Pressing Iron

Given that thermal power of charcoal = 184.68W (earlier calculated based on equation (1.11))

$$\text{Energy input } (E_{\text{in}}) = 184\text{W} \times \left(\frac{1800}{60 \times 60}\right)\text{hr} = 652.5\text{KJ}$$

Useful energy output of the charcoal pressing iron is given by the expression:

$$Q_{\text{out}} = M_T C_T \Delta T;$$

Where: M_T is the mass of linen fabric

C_T is the specific heat capacity of textile and ΔT is the temperature change which is difference between 36°C ambient temperature and 266°C temperature at the end of the cloths ironing process.

$$\begin{aligned} \text{Thus } Q_{\text{out}} &= 1\text{kg} \times 1.90\text{kJ/kgK} \times (230+273.15)\text{K} \\ &= 1\text{kg} \times 1.90\text{kJ/kgK} \times 503.15\text{K} \\ &= 955.985\text{KJ} \end{aligned}$$

Efficiency η

$$= \frac{\text{Network Output}}{\text{Heat Added at High Temperature}}$$

Conversely, for a resistive heat device, efficiency can be expressed thus:

$$\text{Efficiency} = \frac{E_{\text{in}} (\text{KJ})}{Q_{\text{out}} (\text{KJ})} \quad 14$$

$$\text{Efficiency of Traditional Charcoal Pressing Iron } (\eta_{\text{tcpi}}) = \frac{652.5\text{KJ}}{955.985\text{KJ}} = 0.09659 = \mathbf{9.7\%}$$

3.15 Efficiency and Coefficient of Performance of Automated Charcoal Pressing Iron

The efficiency of automated charcoal pressing iron (η_{acpi}) is given by the expression

$$\eta_{acpi} = \frac{E_{in} (KJ)}{Q_{out} (KJ)}$$

The useful energy input (E_{in}) = 1500 x $\left(\frac{1800}{60 \times 60}\right)$ hr
= 750KJ

Energy output which is heat supplied to linen fabric = 955.985KJ (earlier calculated)

$$\eta_{acpi} = \frac{750KJ}{955.985KJ} = 0.78 = 78\%$$

Efficiency of Automated Charcoal Pressing Iron is **78%**.

3.16 Coefficient of Performance (COP)

The concept of COP is not commonly used for a charcoal pressing iron because the system is a simple resistive heating device which energy input is usually converted directly to heat energy used for the cloth ironing activity. In comparison, this automated charcoal pressing Iron is 68.3% more efficient than the traditional charcoal pressing Iron.

Conclusion

This design addresses the cloths ironing needs of people in the rural areas lacking electricity and the utilization of the concurrent engineering approach ensures that design, production and marketing introduction occur in tandem; thus reducing development time. The unit cost of the product including manufacturing, marketing and distribution margins stands at ₦ 17,513.33 per unit with an anticipated annual sales volume of 30,000 units. Comparatively, the unit cost is below that of a standard quality

electric pressing iron which currently sales between ₦18, 000 .00 and ₦ 28,000 .00 per unit and requires electricity which is either limited or completely unavailable in rural areas. The device has better performance and therefore offers comfortable users convenient for cloths ironing chores of every rural household in regions without electricity. This new variant charcoal pressing iron provides an efficient and affordable solution for rural households while ensuring sustainable business growth.

References

- Ajah, N. J. (2018). Performance Evaluation of Waste Heat Recovery in a Charcoal Stove using a thermoelectric Module. *European Journal of Sustainable Development Research* 2(2), 25. <https://doi.org/10.20897/ejosdr/85187>
- Beretta, D., Neophytou, N., Hodges, J. M., Kanatzidis, M. G., Narducci, N. D., Martin-Gonzalez, M., Beekman, M., Balke, B., Cerretti, G., Tremel, W., Zevalkink, A., Hofmann, A. I., Muller, C., Dorling, B., Campoy-Quiles, M., Caironi, M. (2019). Thermoelectrics: From History, A Window To The Future. *Journal of Materials Science Engineering R*, 1381(2019), 100501. <https://doi.org/10.1016/j.mser.2018.09.001>
- Bethan (2022). Laundering Weight Calculator (UK Guide in Uk): In the Wash. <https://inthewash.co.uk>
- Cao, T., Shi, X., Li, M., HU, B., Chen, W., Liu, W., Lyu, W., Macleod, J. and Chen, Z. (2023). Advances In Bismuth – Tellurides – Based Thermoelectric Devices: Progress and Challenges. *Journal of eScience* 3(3). <https://doi.org/10.1016/j.es.2023.100122>

- Fiksel, J. (2009). Design For Environment: A Guide to Sustainable Product Development. 2nd ed. New York: McGraw-Hill.
<https://www.accessengineeringlibrary.com/content/book/9780071605564>
- Goldsmid, H. J. (2014). Bismuth telluride and its Alloys as Material for Thermoelectric Generation. 7(4), 2577 – 2592. <https://doi.org/10.3390/ma7042577>
- Goupil, C., Querdane, H., Zabroki, K., Seifert, W., Hinsche, N. F. and Müller, E. (2016). “Thermodynamics and Thermoelectric”. In Goupil, Christophe (ed.). *Continuum Theory and Modeling of Thermoelectric Elements*. New York: Wiley-VCH. 2-3. ISBN 9783527413379
- Hassan, L. G., Sani, N. A., Sokoto, A. M. & Tukur, U. G. (2017). Comparative Studies of Burning Rates and Water Boiling Time of Wood Charcoal and Briquettes Produces from Carbonized Martynia annua Woody Shells. *Nigerian Journal of Basic and Applied Sciences*. 25(2). <https://doi.org/10.4314/njbas.v25i2.4>
- Hou, W., Nie, X., Zhao, W., Zhou, H., Mu, X., Zhu, W. and Zhang, Q. (2018). Fabrication and Excellent Performance of $Bi_{0.5}Sb_{1.5}Te_3$ /epoxy Flexible Thermoelectric Cooling Devices. *Journal of Nano Energy*. 50(2018), 766-776.
<https://doi.org/10.1016/j.nanoen.2018.06.020>
- Jones, H. G. (1939). The Charcoal Iron Industry: *Journal of the Royal Society of Arts*. 88(4504), 41 – 57.
<http://www.jstor.org/stable/41359471>
- Kim, K. T., Kim, K. J. and Ha, G. H. (2010). Thermoelectric Properties of P – Type Bismuth telluride powder synthesized by a Mechano-Chemical Process. *Electron Mater*. 6(1), 177 – 180.
<https://doi.org/10.3365/eml.2010.12.177>
- Kuroki, T., Kabeya, K., Makino, K., Kajihara, T., Matsuno, H., Fujibayashi, A., H. T. Kaibe, H.T. & Hachiuwa, H. (2014). Thermoelectric Generation Using Waste Heat in Steel Works. *Journal of Electronics Materials* 43(6).
<https://doi.org/10.1007/S11664-014-3094-5>
- Lubwama, M., Yiga, V. A., Ssempijja, I., Lubwama, H. N. (2021). Thermal and Mechanical Characteristics of Local Firewood Species and Resulting Charcoal Produced by Slow Pyrolysis. *Springer Journal: Biomass Conversion and Biofinery*. 13(2023), 6689 – 6704. <https://doi.org/10.1007/s13399-021-01840-2>
- Magé, J-P. (2006). Charcoal Production. *BluKarb: The Charcoal New Generation*. GIZ HERA Cooking Energy Compendium. *A Practical Guidebook for Implementers of Cooking Energy Intervention*.
<https://www.blukarb.com/english/>
- Mcgril, J (2017). The History of Charcoal Iron Presses. *Oureverydaylife.com*. <https://oureverydaylife.com/the-history-of-coal-iron-presses-12296849.html>
- Nurba, D., Yasar, M., Mustaqimah, R., Fadhil, S., Sari, P. & C. V. Maysa, C. V. (2019). Performance of Corncobs and Wood Charcoal Briquette as Heat Energy Sources in In-Store Dryer. *IOP Conference Series: Earth and Environmental Science* 365(2019) 012048. <https://doi.org/10.1088/1755-1315/365/1/012048>
- Olusegun, A. S. & Ijagbemi, C. O. (2014). Performance Evaluation of Charcoal Samples from Different Wood Species in Ibadan, Nigeria. *Journal of Engineering and Applied Scientific Research*. 6(1), 50 – 56. <https://doi.org/10.9790/3021-04465764>
- Opensaw, K. (2009). Annex III – (b) Measuring Fuelwood and Charcoal.

- Retrieved from <https://www.fao.org/3/X5328e/x5328e05.htm#4.1.%20how%20wood%20is%20transformed%20into%20charcoal>
- Rabiu, T. O., Yekinni, A. A. and Lamidi, S. B. (2020). Production of Electrical Energy Through Thermoelectric Effect: *International Journal of Modern Engineering Research (IJMER)*, 10(01), 2019, 01-07. <https://scholar.google.com>
- Sestak, J. (2005). Understanding Heat, Temperature and Gradients. *Science of Heat and Thermophysical Studies. A General Approach to Thermal Analysis*. 140-167. <https://doi.org/10.1016/B978-044451954-2/50005-9>
- Sharper, N. M., Zhmakin, L. I. & Osmanov, Z. N. (2017). A Study of the Heat Capacity of Textile Materials. *Fibre Chem.* 48 (2017). 515 – 518. <https://doi.org/10.1007/s10692-017-9829-3>
- Shuaiwai.com. <https://www.shuaiwei.com/news/industry-nes/whats-is-the-temperature-of-the-iron-during-normal-operation.html#>
- Soumi, A. I., Utomo, B. R., Partono, R. P., Tjahjono, T., Atmoko, N. T. and Sulistyanto, A. (2023). Performance of Thermoelectric Generator in the Combustion of Wood Charcoal with Various Fan Powers. *The 6th Mechanical Engineering Science and Technology International Conference (MEST 2023, AER 222)*, 210 – 219. https://doi.org/10.2991/978-94-6463-134-0_20
- Spenser-Smith, J. L. (2008). The Specific Heat of Hygroscopic Textiles. *The Journal of the Textile Institute*. 61(4), 194 – 196. <https://doi.org/10.1080/00405007008660035>
- Snyder, G. J. and Snyder, A. H. (2017). Figure of Merit ZT of A Thermoelectric Device Defined From Materials Properties. *Journal of Energy & Environmental Science*. 10(2017), 228-2283. <https://doi.org/10.1039/C7EE02007D>
- Tecpro (n.a). <https://www.tegmart.com/thermoelectric-modules/>
- The Engineering ToolBox (2003). *Solids – Specific Heats*. Retrieved from: https://www.engineeringtoolbox.com/specific-heat-solids-d_154.html
- Wu, F., Wang, W., Hu, X. and Tang, M. (2017). Thermoelectric properties of I – doped n-type Bi₂Te₃–based material prepared by hydrothermal and subsequent hot pressing progress in *Natural Science: Materials International* 27(2), 203 – 207. <https://doi.org/10.1016/j.pnsc.2017.02.009>
- Zhang, X. and Zhao, L. (2015). Thermoelectric Materials: Energy Conversion between Heat and Electricity. *Journal of Materiomics*. 1(2), 92-105. <https://doi.org/10.1016/j.jmat.2015.01.001>